journal of the mechanical behavior of biomedical materials 143 (2023) 105888

Contents lists available at ScienceDirect

Journal of the Mechanical Behavior of Biomedical Materials

journal homepage: www.elsevier.com/locate/jmbbm

Development of Y-TZP/MWCNT-SiO_2 nanocomposite for dental protheses

Lucas Hian da Silva [a], Laura Ajamil Rinaldi [a], Dolores Ribeiro Ricci Lazar [b], Valter Ussui [b,1], Rubens Nisie Tango [c], Renan Belli [d], Ulrich Lohbauer [d], Paulo Francisco Cesar [a,*]

[a] Department of Biomaterials and Oral Biology, Faculty of Dentistry, Universidade de São Paulo (USP), Brazil
[b] Materials Science and Engineering Center, Nuclear and Energy Research Institute (IPEN), Brazil
[c] Departamento of Dental Materials and Prosthodontics, Institute of Science and Technology (ICT), Universidade Estadual Paulista "Júlio Mesquita Filho" (UNESP), Brazil
[d] Research Laboratory for Dental Biomaterials, Dental Clinic 1, Friedrich-Alexander-Universität Erlangen-Nürnberg (FAU), Germany

ARTICLE INFO

Keywords:
Yttria-stabilized tetragonal zirconia polycrystals
Multi-walled carbon nanotube
Hydrothermal treatment
Co-precipitation of mixed hydroxides

ABSTRACT

Y-TZP/MWCNT-SiO_2 nanocomposite was synthesized by co-precipitation and hydrothermal treatment methods. After the characterization of the MWCNT-SiO_2 powder, specimens were obtained from the synthesized material Y-TZP/MWCNT-SiO_2 by uniaxial pressing for a second characterization and later comparison of its optical and mechanical properties with the conventional Y-TZP. The MWCNT-SiO_2 was presented in bundles of carbon nanotubes coated by silica (mean length: 5.10 ± 1.34 μm /D90: 6.9 μm). The composite manufactured was opaque (contrast ratio: 0.9929 ± 0.0012) and had a white color with a slightly difference from the conventional Y-TZP (ΔE_{00}: 4.4 ± 2.2) color. The mechanical properties of Y-TZP/MWCNT-SiO_2: vickers hardness (10.14 ± 1.27 GPa; $p = 0.25$) and fracture toughness (4.98 ± 0.30 MPa $m^{1/2}$; $p = 0.39$), showed no significant difference from the conventional Y-TZP (hardness: 8.87 ± 0.89; fracture toughness: 4.98 ± 0.30 MPa $m^{1/2}$). However, for flexural strength ($p = 0.003$), a lower value was obtained for Y-TZP/MWCNT-SiO_2 (299.4 ± 30.5 MPa) when compared to the control Y-TZP (623.7 ± 108.8 MPa). The manufactured Y-TZP/MWCNT-SiO_2 composite presented satisfactory optical properties, however the co-precipitation and hydrothermal treatment methods need to be optimized to avoid the formation of porosities and strong agglomerates, both from Y-TZP particles and MWCNT-SiO_2 bundles, which lead to a significant decrease in the material flexural strength.

1. Introduction

Among several types of ceramics used to produce dental prostheses, yttria-stabilized tetragonal zirconia polycrystal (Y-TZP) stands out due its high fracture toughness (7 to 10 MPa $m^{1/2}$) compared to other dental ceramics such as feldspathic porcelains, glass-ceramics, pollycritalline alumina and glass-infiltrated composites (Larsson et al., 2007). Y-TZP displays an important toughening mechanism related to the martensitic transformation of crystalline grains that result in the high fracture toughness values obtained in laboratorial tests (Larsson et al., 2007; Manicone et al., 2007; White et al., 2005; Pittayachawan et al., 2009). Due to the good mechanical properties, Y-TZP has been indicated for structural uses associated to high mechanical stresses as in the case of multiple fixed partial dentures of up to six dental elements and aesthetic abutments applied over dental implants (Pittayachawan et al., 2009; Tinschert et al., 2001). Before the release of Y-TZP in the dental market, the use of dental ceramics in these clinical situations was not considered safe due high incidence of fracture events (Manicone et al., 2007; McLaren and Giordano, 2005; Mitsias et al., 2010).

As a result of the evolution of nanotechnology, new materials have been developed, such as carbon nanotubes (CNT), which can have a single layer (sigle wall - SW) or multiple layers with a tubular format (multi wall - MW). Carbon nanotubes are derived from fullerene, a crystalline allotropic form of carbon with high stability that can be used for the synthesis of several chemical compounds. Amongst all materials currently available, CNT is considered the one with the best mechanical properties, with tensile strength of up to 63 GPa and elastic modulus around 950 GPa (Ando, 2010; Yu et al., 2000). One study (Popov et al., 2002) demonstrated that the hardness of these nanotubes varies from 62 to 150 GPa, being close to the hardness of the diamond (150 GPa). After the discovery of these excellent properties of CNT, multiple studies have emerged proposing their use to reinforce ceramic and metallic materials

* Corresponding author. Department of Biomaterials and Oral Biology - FOUSP, Av. Prof. Lineu Prestes, 2227 - Butantã, 05508-000, São Paulo, SP, Brazil.
E-mail address: paulofc@usp.br (P.F. Cesar).
[1] In memoriam.

https://doi.org/10.1016/j.jmbbm.2023.105888
Received 10 March 2023; Received in revised form 1 May 2023; Accepted 3 May 2023
Available online 4 May 2023

(Curtin and Sheldon, 2004).

The addition of carbon nanotubes to Y-TZP with the objective of increasing its longevity and reliability has been previously reported. One report on the properties of a Y-TZP/MWCNT (multi-walled carbon nanotubes) composite showed high values of fracture toughness and hardness compared to a control Y-TZP (Garmendia et al., 2010a). In this same study, the stress intensity factor threshold (K_{I0}) was also evaluated, indicating that the carbon nanotube composite showed a K_{I0} value that was 15% higher (4.4 ± 0.1 MPa $m^{1/2}$) compared to the conventional Y-TZP (3.8 ± 0.1 MPa.$m1^{/2}$). This increase was attributed to the influence of toughing mechanisms related to the presence of CNT in the material, such as crack-bridging. Crack-bridging is a mechanism that takes place at the crack wake where bridges are formed between both surfaces of the crack, hindering its propagation.

Further studies showed that the incorporation of CNT to Y-TZP delays the decomposition of the monoclinic phase during sintering, reduces grains growth in the microstructure and increases density of the material (Garmendia et al., 2010b, 2012). Despite the excellent results reported in the literature, it is important to note that the final composite obtained in these experiments had a dark gray color due to the dark shade of the CNT, thus preventing its use in dental applications due to the unacceptable aesthetic result for a restoration. A possible solution to this problem has recently emerged with the development of functionalized carbon nanotubes (Jagadeesan and Eswaramoorthy, 2010).

The functionalization process consists of attaching different chemical elements to the atoms on the material's surface (adsorption of functional groups), which change the rheology of suspensions formed from CNTs, broadening the range of applications for these materials. Functionalization can also promote better dispersion of the nanotube in the material matrix (Jagadeesan and Eswaramoorthy, 2010). CNT functionalized with silica has a white shade and, therefore is an good candidate material to be used in dental restorations.

The main objective of this study was to evaluate and characterize the synthesis of a ceramic nanocomposite containing carbon nanotubes coated with silica (Y-TZP/MWCNT-SiO_2). The secondary objective was to develop a Y-TZP/MWCNT-SiO_2 nanocomposite with mechanical and optical properties that could allow its future use as infrastructure for fixed dental prostheses and implant abutments for CAD-CAM systems. For that reason, this study evaluated the microstructure, flexural strength, fracture toughness and optical properties of the nanocomposite and compared these properties with those measured for conventional Y-TZP.

2. Materials and methods

2.1. Characterization of MWCNT-SiO_2

Prior to the start of composite synthesis, the silica coated multi-walled carbon nanotube (MWCNT-SiO_2, Nanoshell LLC, USA) was characterized in terms of its morphology, dimension, thermal stability and composition.

For analysis using scanning electron microscopy (SEM-FEG) and transmission electron microscopy (TEM), the material powder was dispersed in a solution of butyl alcohol with the aid of ultrasound (Kondentech Indústria e Comércio Ltda. - EPP, São Carlos-SP, Brazil) to avoid cluster formation. After approximately 5 min of dispersion, the suspension produced was applied with a fine brush on the stub for the SEM-FEG JSM 6701S (JEOL, Tokyo, Japan) and on 200 meshes copper screens covered with a film polyvinyl formalin (Formvar, Shawinigan Resins Corp., Massachusetts, USA) for TEM JEM 1010 (JEOL, Tokyo, Japan). For the calculation of the average length of the MWCNT-SiO_2, the photomicrographs obtained in SEM-FEG were taken to the software IMAGE J 1.32 in which they were binarized and received treatment according to ASTM E-1382 (1997) (Standard Test Methods for Determining, 2002) for the measurements of the length.

A thermogravimetric analysis (TGA) was performed on air atmosphere for the MWCNT-SiO_2 in order to verify up to what temperature it would maintain its structural stability. X-ray diffraction (XRD 7000, Shimadzu do Brasil, São Paulo - SP, Brazil) from MWCNT-SiO_2 was performed before and after the calcination process that takes place during TGA, in order to identify the possible components in the material and what losses would be observed after calcination. The identification of the peaks observed in the diffractogram was made using the ICDD (International Center for Diffraction Data) forms. In order to confirm and reinforce the identification of the peaks observed in the diffractograms, an X-ray fluorescence spectroscopy (XRF) was also performed for the MWCNT-SiO_2 and for the residue after the TGA.

2.2. Synthesis of the Y-TZP/MWCNT-SiO_2 nanocomposite

Coating of the MWCNT-SiO_2 with zirconium oxide stabilized by yttrium oxide was performed by hydrothermal treatment using as precursors the zirconium and yttrium hydroxides co-precipitated in a solution containing MWCNT-SiO_2. The co-precipitation of mixed zirconium and yttrium hydroxides was performed previously with 3 M ammonium hydroxide, fixing the concentration of oxides, zirconium oxychloride (zirconium oxychloride, IPEN - USP Laboratory) and yttrium chloride (chloride of yttrium, Sigma - Aldrich), in the starting solution at 35 $g.L^{-1}$. To guarantee maximum hydroxide precipitation, the pH value was kept at 10. The precipitates obtained were filtered and washed with distilled water until the elimination of chloride ions. Mass concentrations of 4 g for dry and disaggregated mixed hydroxides and 75 mg of MWCNT-SiO_2 were standardized (Garmendia et al., 2008). Using an ultrasonic bath equipment, the powders were dispersed in a solution containing 50 ml of ammonium hydroxide P.A. (Merck Brasil, Cotia – SP, Brazil) and 50 ml of deionized water for hydrothermal treatment. The precipitates obtained after the hydrothermal treatment were filtered and washed in distilled water to remove the formed salts. After washing, the powders were dried in an oven at a temperature of ~80 °C for 24 h and in a furnace Series FC (EDG Equipamentos, São Paulo - SP, Brazil) at 120 °C for 1 h.

All dry powders obtained in the described processes were manually disaggregated in an agate mortar and subjected to analysis by SEM-FEG and TEM to observe and confirm the coating of the MWCNT-SiO_2 by the ceramic particles.

To produce the nanocomposite (Y-TZP/MWCNT-SiO_2), zirconia ceramic powder stabilized with 3 mol% of yttria without binder (TZ-3Y-E, Tosoh Corporation, Tokyo, Japan) was added, plus 1 vol% of MWCNT-SiO_2 coated with yttria stabilized zirconia particles obtained by hydrothermal treatment process without the use of organic liquids. The mixture was carried out in a ball mill (Pulverisette 5, Fritsch, Idar-Oberstein, Germany) for 16 h using zirconia spheres and deionized water as the vehicle, with approximately 50 mass% of the mixture being solid. After grinding, the powder was dried in a FANEM 520 oven at 80 °C for 24 h and in a furnace Series FC (EDG Equipamentos) at 120 °C for 1 h for further disaggregation in an agate mortar.

2.3. Specimen production

Using the ceramic composite Y-TZP/MWCNT-SiO_2 powder, disk-shaped specimens were formed with a diameter of 15 mm and a thickness of 2 mm by uniaxial pressing at 67 MPa. These specimens were used to evaluate the optical properties and fracture toughness of the material. Prior to the proposed tests, the samples were subjected to the sintering cycle carried out in an argon atmosphere tubular furnace (SPX Thermal Product Solutions, White Deer - PA, USA) at 1,400 °C for 4 h with a heating rate of 5 °C/min.

To evaluate the flexural strength, bar-shaped specimens were made by uniaxial hydraulic pressing (MPH-15, Marcon Indústria Metalúrgica Ltda., Marília - SP, Brazil) using a stainless steel matrix, where the powders were subjected to a pressure of 67 MPa for 30 s to form blocks (n = 3) in the green state of the Y-TZP/MWCNT-SiO_2 composite and TZ-

3Y-E. The blocks partial sintering of the two materials (Y-TZP/MWCNT-SiO_2 and TZ-3Y-E) was carried out in a Lindberg tubular oven with an argon atmosphere (SPX Thermal Product Solutions, White Deer - PA, USA) at a temperature of 1,100 °C for 1 h with a heating rate of 5 °C/min. The partially sintered TZ-3Y-E and Y-TZP/MWCNT-SiO_2 blocks were sectioned on a precision saw machine (Isomet, Buehler, Lake Bluff-IL, USA) by 15HC diamond discs (Buehler, Lake Bluff-IL, USA) with abundant irrigation to obtain bar-shaped samples. The final sintering cycle was carried out in a tubular furnace in argon atmosphere at 1,400 °C for 4 h with a heating rate of 5 °C/min. The bar-shaped specimens, after final sintering, were 25 mm-long, 4 mm-wide and 3 mm-thick, with its four longest corners chamfered according to ISO 6872: 2008 (Dentistry, 2008).

2.4. Evaluation of the optical properties

The CM 3700d spectrophotometer (Konica Minolta Sensing, Inc., Osaka, Japan) was used to evaluate the optical behavior of the materials, operating in the visible light wavelength range (400 to 700 nm). The mirror polished specimens in automatic polisher (Automet, Buehler, Lake Bluff-IL, USA) of both materials ($n_o = 3$) were analyzed to obtain reflectance values on white and black backgrounds, in addition to total transmittance. With these data, it was possible to obtain contrast ratio values and the color difference (ΔE) between the materials.

The contrast ratio (RC) is the optical property that measures the transparency or opacity of a material, being measured by the ratio between the reflectance of the sample on a black background (Y_p) and a white background (Y_b). Applying the values obtained in the spectrophotometer in equation (Larsson et al., 2007), it is calculated:

$$RC = \frac{Y_p}{Y_b} \tag{1}$$

The color difference between the composite Y-TZP/MWCNT-SiO_2 and the TZ-3Y-E was verified by measuring the color difference parameter (ΔE_{00}). The ΔE_{00} was obtained by measuring the parameters L*, a* and b* of the CIELab system (CIEDE2000) in transmittance mode for each material, Y-TZP/MWCNT-SiO_2 and TZ-3Y-E, and following equation (Manicone et al., 2007) it is calculated:

$$\Delta E_{00} = \left[\left(\frac{\Delta L'}{K_L S_L} \right)^2 + \left(\frac{\Delta C'}{K_C S_C} \right)^2 + \left(\frac{\Delta H'}{K_H S_H} \right)^2 + R_T \left(\frac{\Delta C'}{K_C S_C} \right) \left(\frac{\Delta H'}{K_H S_H} \right) \right]^{\frac{1}{2}} \tag{2}$$

Where ΔL', ΔC', and ΔH' are the differences in lightness, chroma and hue between Y-TZP/MWCNT-SiO_2 and TZ-3Y-E. *SL*, *SC*, and *SH* are the weighting functions for the lightness, chroma, and hue components. *KL, KC, KH* are the correction terms to be adjusted according the experimental conditions, in this study, they were set at 1.

The *RC* of each material was compared using the Student's *t*-test ($\alpha = 0.05$). The limit value of the color difference (ΔE_{00}) was established at 3.48 (Ghinea et al., 2010), with values below these being difficult to detect by human eye without proper training for a clinical situation in an oral environment.

2.5. Fracture toughness evaluation

Pellet-shaped specimens for the two materials (n = 3) were used and, in each specimen, four Vickers indentations were performed. The indentation load was established at 20 kgf with an application time of 20 s for both materials, thus guaranteeing the occurrence of a median/radial crack with a relation between the crack size (c) and half the diagonal of the Vickers indentation (a) (c/a ratio) close to 2. This type of crack allowed the use of equation (White et al., 2005) by Niihara et al. (1982) (Niihara et al., 1982) to calculate fracture toughness (stress intensity factor in opening mode, or mode I):

$$K_{Ic} = 0,067 \left(\frac{E}{H} \right)^{2/5} Ha^{1/2} \left(\frac{c}{a} \right)^{-3/2} \tag{3}$$

where, *a* is half the indentation diagonal, *c* is the crack size, *H* is the Vickers hardness, and *E* is the modulus of elasticity. The Vickers hardness (GPa) and fracture toughness ($MPa.m^{1/2}$) of each material were calculated using the means of the 4 indentations performed on the 3 specimens, which were statistically analyzed using the Student *t*-test ($\alpha = 0.05$) to check for significant differences.

2.6. Evaluation of flexural strength

The bar-shaped specimens of Y-TZP/MWCNT-SiO_2 and TZ-3Y-E (n = 5) were fractured immersed in distilled water at 37 °C in a 4-point bending test following the recommendations of ISO 6872: 2008 (Dentistry, 2008). The specimens of both materials were positioned in devices created for the test, in order to guarantee perfect alignment and providing uniform contact of the spherical spans with a standardized diameter of 2.4 mm. The test was performed on a DynaMess TP 5 kN HF machine (DynaMess, Aachen, Germany) with a loading speed of 0.5 mm/min.

The data obtained were subjected to statistical analysis using the Student's *t*-test with a 5% significance level ($\alpha = 0.05$). After the mechanical test, a fractographic analysis was performed and scanning electron microscopies (SEM) were performed on the fracture surfaces of the tested specimens with the intention of observing possible microstructure defects and the probable region of the fracture origin.

3. Results

3.1. Characterization of MWCNT-SiO_2

The photomicrographs obtained by SEM-FEG (Fig. 1) indicated that the MWCNT-SiO_2 formed bundles from a set of carbon nanotubes apparently with the surface coated with SiO_2.

The photomicrographs obtained by TEM also showed the morphological aspects of MWCNT-SiO_2. However, the presence of other particulate matter of smaller dimensions than the carbon nanotube was noted (Fig. 2). Such particles were identified as being silica (SiO_2) in subsequent analyzes (TGA, DRX and FRX). The MWCNT-SiO_2 had an average length of 5.10 ± 1.34 μm, for a total of 100 measured bundles. Of all 100 bundles, 90% of the measured lengths (D90) were below 6.9 μm.

Thermogravimetric analysis (TGA) showed that little loss of mass occurred up to a temperature of 1,400 °C, resulting in a loss of only 20% of the initial mass (Fig. 3). This result indicates the presence of other compounds with higher thermal resistance in the material, in addition to carbon nanotubes (MWCNT).

The diffractograms obtained by XRD showed that the MWCNT-SiO_2 before calcination showed a long peak at 22° of 2θ (Fig. 4). After the calcination process, it was observed the formation of high intensity peaks indicating that the material underwent strong crystallization. The identification of the peaks in the ICDD (International Center for Diffraction Data) sheets showed that these peaks coincided with the compound silicon dioxide (SiO_2) in the crystalline form of cristobalite.

The X-ray fluorescence (XRF) analysis for the MWCNT-SiO_2 and for the residue after the TGA confirmed, from the observed concentrations and compounds (Table 1), that most of the substances that make up the MWCNT-SiO_2 would be silicon dioxide (SiO_2), which undergoes crystallization to cristobalite after the calcination process. However, XRF spectroscopy is not able to detect carbon.

3.2. Characterization of the Y-TZP/MWCNT-SiO_2 nanocomposite

The SEM-FEG and TEM analysis of the MWCNT-SiO_2 powder after

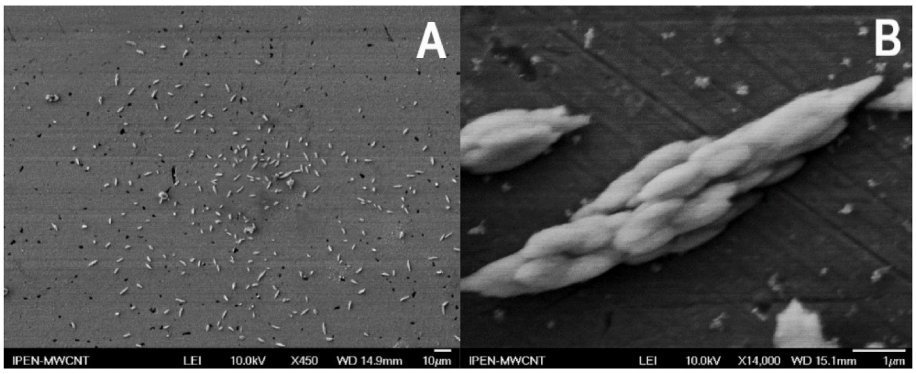

Fig. 1. (A) Photomicrography using SEM-FEG of several MWCNT-SiO_2. (B) Photomicrography using SEM-FEG of a single MWCNT-SiO_2.

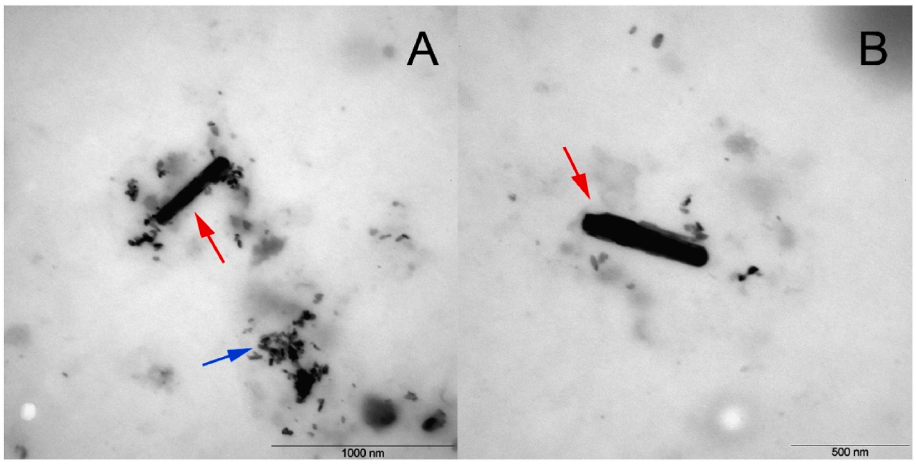

Fig. 2. Photomicrography using TEM of two MWCNT-SiO_2 in different magnifications. Red arrows indicating the MWCNT-SiO_2 and blue arrow indicating the presence of silica.

hydrothermal treatment without the use of organic liquids revealed that this processing route was effective in providing the coating of the carbon nanotube by particles of zirconium and yttrium oxide (Fig. 5). However, processing from co-precipitation to hydrothermal synthesis using exclusive water caused the formation of agglomerates and Y-TZP particles larger than 5 µm (Fig. 6).

3.3. Evaluation of optical properties

There was a significant color difference between the materials Y-TZP/MWCNT-SiO_2 and TZ-3Y-E, with an ΔE_{00} of 4.4 ± 2.2. Both materials showed a white color and high opacity according to the results measured for *RC* (Table 2), however there was statistical difference

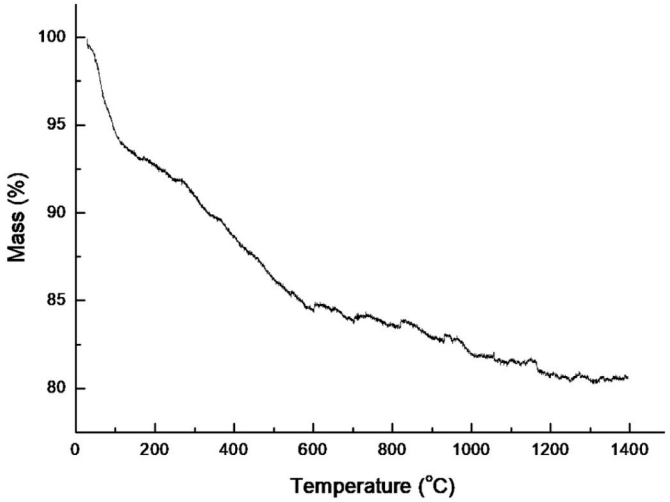

Fig. 3. TGA graph for MWCNT-SiO_2.

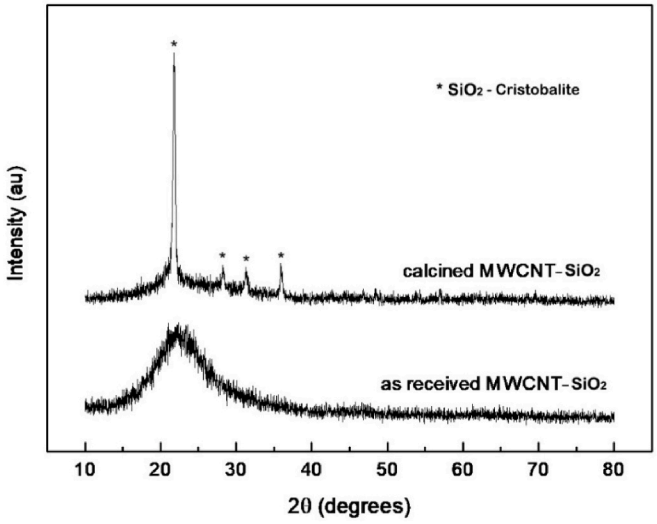

Fig. 4. MWCNT-SiO_2 diffractograms obtained by XRD before and after calcination performed in the TGA.

Table 1
Results of chemical analysis by XRF of MWCNT-SiO_2.

Oxide	Concentration (%)	
	MWCNT-SiO_2	MWCNT-SiO_2 after calcination
SiO_2	96.757	98.118
Al_2O_3	2.498	1.753
SO_3	0.689	0.044
Fe_2O_3	0.056	0.081
MoO_3	————	0.002

*carbon detection by XRF was not possible.

between the values obtained (p = 0.000). TZ-3Y-E presented itself as an opaquer material when compared to Y-TZP/MWCNT-SiO_2. The measurements of the parameters L*, a* and b* of the composite Y-TZP/MWCNT-SiO_2 and TZ-3Y-E are shown in Fig. 7. The increase in parameter L* for the composite Y-TZP/MWCNT-SiO_2 in comparison with conventional Y-TZP (TZ-3Y-E) indicates greater luminosity, being characterized as a lighter material. The increase of the parameter a* in the composite shows that it underwent a reddening compared to TZ-3Y-E, however still maintaining the greater presence of green, since the value is negative. For parameter b*, there was a decrease in the values of the composite when compared to that of conventional Y-TZP, corresponding to decrease in the amount of the yellow in the material.

3.4. Evaluation of fracture toughness

The mechanical properties of Y-TZP/MWCNT-SiO_2, Vickers hardness (10.14 ± 1.27 GPa; p = 0.25) and fracture toughness (4.98 ± 0.30 MPa $m^{1/2}$; p = 0.39), showed no significant difference compared to the conventional Y-TZP (hardness: 8.87 ± 0.89 GPa; fracture toughness: 4.98 ± 0.30 MPa $m^{1/2}$) (Table 3). Although there was no statistical difference between Vickers hardness (p = 0.25) and fracture toughness (p = 0.39) between Y-TZP/MWCNT-SiO_2 and TZ-3Y-E by the Vickers indentation test, evidence of the presence of a toughening mechanism was verified for the ceramic composite developed, since most of the indentations made on this material showed a very small or none crack formation, however these were not considered for the fracture toughness calculation.

3.5. Evaluation of flexural strength

In the flexural strength test, statistically lower values (p = 0.003) were obtained for the experimental material Y-TZP/MWCNT-SiO_2 (299.4 ± 30.5 MPa) when compared to the control TZ-3Y-E (623.7 ± 108.8 MPa) (Table 4). However, a lower relative standard deviation was

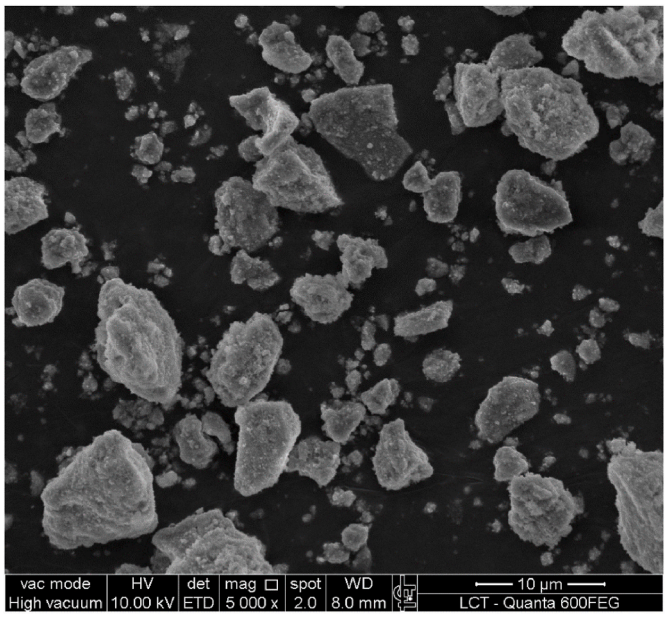

Fig. 6. Photomicrography using SEM-FEG of the MWCNT-SiO_2 powder after hydrothermal treatment without the use of organic liquids to coat the carbon nanotubes. Photomicrograph showing the size of zirconium oxide and yttrium particles.

observed for the experimental composite (10%) when compared to the TZ-3Y-E (17%).

Fractographic analysis of fractured bar-shaped specimens using SEM showed that, for both materials, the origin of the fracture occurred at the extremity that was being subjected to tensile stresses (Fig. 8). The origins were identified as surface defects probably created during the sectioning of samples in a precision saw machine.

Photomicrographs of the fracture surface of the Y-TZP/MWCNT-SiO_2 bar-shaped specimen in higher magnification revealed that the MWCNT-

Table 2
Contrast ratio for studied materials.

Material (n = 3)	Contrast Ratio (RC)
TZ-3Y-E	0.9967 ± 0.0024 A*
Y-TZP/MWCNT-SiO_2	0.9929 ± 0.0012 B*

*Different letters represent a statistically significant difference at the 5% level using the Student's *t*-test.

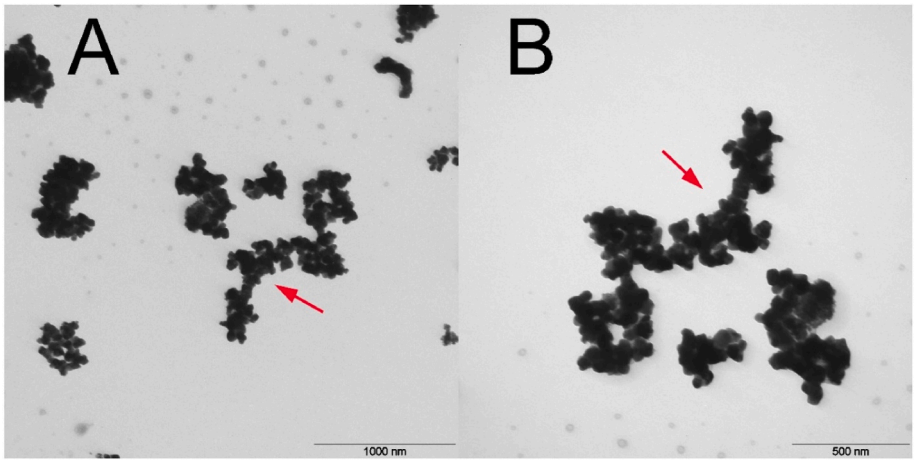

Fig. 5. TEM photomicrographs of the MWCNT-SiO_2 powder after hydrothermal treatment without the use of organic liquids showing the coating of the carbon nanotube by particles of zirconium and yttrium oxide (red arrow).

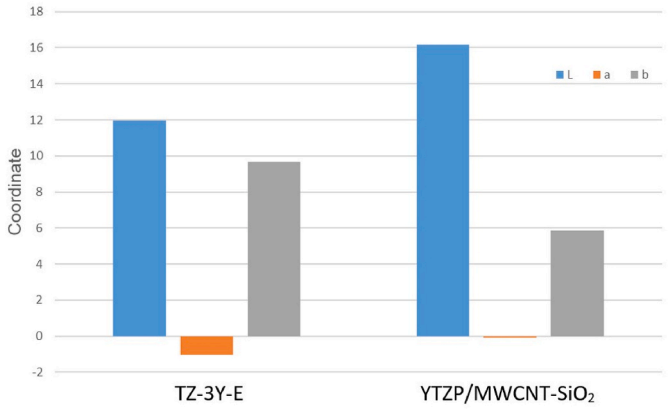

Fig. 7. L*, a* and b* parameters measured for both materials.

SiO_2 was not efficiently dispersed in the Y-TZP matrix (Fig. 9). Furthermore, porosities were also observed in the microstructure of the experimental composite Y-TZP/MWCNT-SiO_2, which may be due to processing problems during the production of the Y-TZP powder (Fig. 10). This high concentration of porosity was not observed in the bars of the TZ-3Y-E control material.

4. Discussion

The results of this study demonstrated the possibility of creating a Y-TZP nanocomposite with the addition of carbon nanotubes (multi-wall) for dental applications, since the developed composite (Y-TZP/MWCNT-SiO_2) showed a white shade and acceptable optical properties for use as dental restorations. However, the problems observed in some of the evaluated mechanical properties must still be better understood in order to seek solutions for the development of the composite with properties that are acceptable for clinical use.

The multi-walled carbon nanotubes (MWCNT) used in this study had different morphological characteristics in comparison with the literature reports for these materials. MWCNT are presented as coaxial cylinders with several layers and with an internal diameter on a nanometric scale, with the outer layers of the nanotube varying in numbers from 2 to 50 (Ando, 2010; Iijima, 1991). In addition, the literature shows photomicrographs of these MWCNT where it is possible to identify each nanotube individually and, in many cases, entangled clusters of them (Ando, 2010; Yoshinori et al., 1998). In present study, the MWCNTs showed a bundle format, as also described by the manufacturer, which corresponds to several MWCNT stacked together. It is believed that such packaging of the carbon nanotubes occurred due to the coating process used during manufacturing of white MWCNTs.

The steps of the coating process carried out by the manufacturer to produce the MWCNT used in this study were not available in details, however, the silica identified in this material indicates that the coating may have resulted in the peculiar aspect of a bundle with a "rice grain" shape and white color. An important problem related to the shape of the material in a "rice grain" bundle is its reduced length when compared to that of conventional MWCNT. The MWCNT bundle used in this study had an average length of 5.10 ± 1.34 μm, but the literature shows that the MWCNTs have longer lengths (10 to 140 μm) when the purpose is to apply this material to improve the toughening mechanisms of ceramics (Garmendia et al., 2010a; Hsieh et al., 2011).

The commercial material purchased (MWCNT-SiO_2), after being subjected to thermogravimetric analysis, showed a mass loss of only 20% in relation to the initial mass when reaching a temperature of 1,400 °C. This result can be explained in two ways. Firstly, there is the fact that this material is mostly composed of silica and only 20% of the powder corresponds to carbon nanotubes. Considering that MWCNT starts to lose its thermal stability at a temperature of 727 °C, it is possible

Table 3
Fracture toughness and Vickers hardness obtained for the studied materials.

Material (n = 3)	Fracture Toughness (MPa.m$^{1/2}$)	Vickers Hardness (GPa)
Y-TZP/MWCNT-SiO_2	4.98 ± 0.30 A*	8.87 ± 0.89 A*
TZ-3Y-E	4.63 ± 0.52 A*	10.14 ± 1.27 A*

*Equal letters in the same column represent statistical similarity with a 5% significance level using the Student's *t*-test.

that all nanotubes have degraded at 1,400 °C (Liew et al., 2005). The second and least likely possibility for this mass loss of only 20% after calcination in the TGA test, is that the MWCNT, after undergoing the coating process, would have strongly integrated into the silica, forming a compound with greater thermal resistance than the conventional MWCNT (Johnson, 1950; Peining et al., 2011). Therefore, this compound did not fully degrade at the temperature of 1,400 °C. In this case, the only part that degraded was that without C-SiO_2 bonds (20%).

It is important to highlight that alcohols were not used in the co-precipitation processes of the precursor hydroxides and thermal synthesis of Y-TZP during the coating of MWCNT-SiO_2 because zirconium oxide has the ability to adsorb molecules of alcohols, water, acetates and acids due to the primary and secondary chemical bonds present in the crystal that attract the molecules of the compounds described (Pearce and Rice, 1928). The impossibility of using alcohols occurs because after their molecules are adsorbed by the material both in the co-precipitation phase and in thermal synthesis, they cannot be eliminated during the sintering of ceramics in an inert atmosphere performed to prevent the MWCNTs from undergoing degradation during this process (Curtin and Sheldon, 2004). Failure to eliminate these molecules adsorbed by the ceramics causes darkening (as seen in the pilot study), making the application of this material in Restorative Dentistry impossible.

Regarding the optical properties, the color obtained for the experimental composite Y-TZP/MWCNT-SiO_2 was considered acceptable so that it can be indicated for the production of dental restorations. Even though the color difference ($\Delta E_{00} = 4.4 \pm 2.2$) between the composite and the conventional Y-TZP was significant, that is, subject to perception by the human eye in a clinical situation ($\Delta E_{00} = 3.48$) (Ghinea et al., 2010), the final color of the composite was within what is acceptable for a restorative material (L* 16.16; a* -0.102; b* 5.86). It is also believed that this Y-TZP composite with MWCNT-SiO_2 may have its high opacity ($RC = 0.9929 \pm 0.0012$) reduced by controlling the growth of grains in the sintering process, which will allow the material to be indicated for monolithic restorations (full-contour) (Zhang and Kim, 2009; Kim et al., 2013) associating the use of dyes to obtain the desired aesthetic (Zhao et al., 2013). Further studies are necessary to prove this concept.

Currently, it is known that ceramic materials that have crystalline microstructure with grains on a nanometric scale and homogeneous sizes have better mechanical properties and greater clinical longevity compared to materials with larger grains (Chen and Xue, 1990; Szepesi and Adair, 2011). However, in the current investigation, the absence of alcohols in the synthesis process of Y-TZP caused a strong agglomeration of the dust particles and an increase in the size of the Y-TZP particles to a micrometric scale. Previous authors (Lazar et al., 2008) demonstrated that the use of alcohols in the synthesis steps of Y-TZP is essential to obtain a good quality powder, since alcohol provides the breakdown of strong agglomerates, reducing grain growth (Lazar et al., 2008).

The present study also showed that the addition of nanotubes in the

Table 4
4-point flexural strength for the studied materials.

Material (n = 5)	Flexural Strength (MPa)
Y-TZP/MWCNT-SiO_2	299.4 ± 30.5 B*
TZ-3Y-E	623.7 ± 108.8 A*

*Different letters represent a statistically significant difference at the 5% level using the Student's *t*-test.

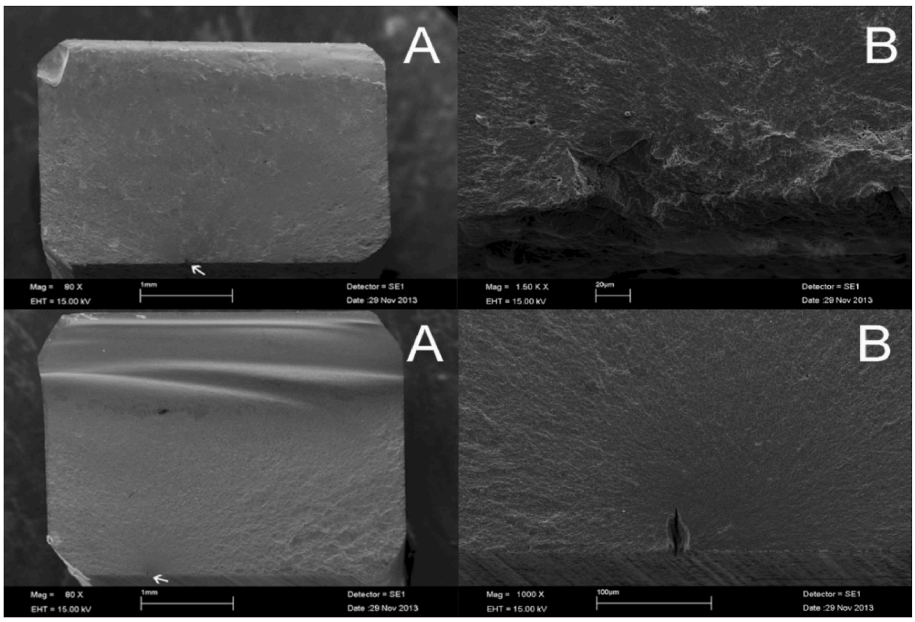

Fig. 8. Photomicrography using SEM of the fractured bar-shaped specimens of Y-TZP/MWCNT-SiO_2 (top A and B) and TZ-3Y-E (bottom A and B). (A) white arrow indicating the fracture origin. (B) Fracture Origin in higher magnification.

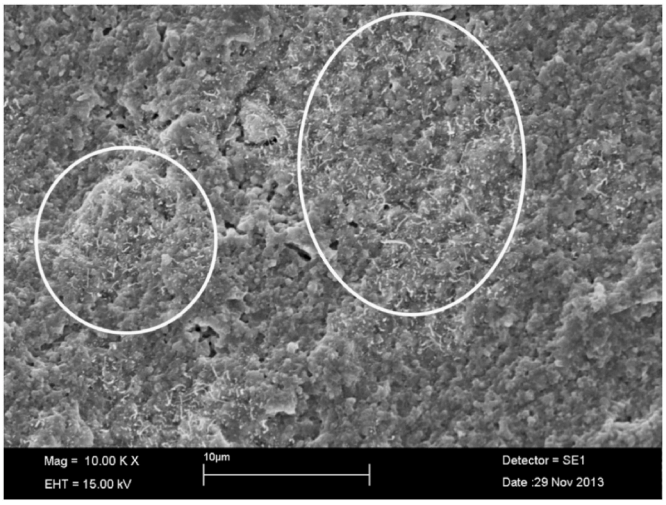

Fig. 9. Photomicrography by SEM of the fracture surface of the Y-TZP/MWCNT-SiO_2 bar-shaped specimen; white ellipses indicating MWCNT-SiO_2 agglomeration regions.

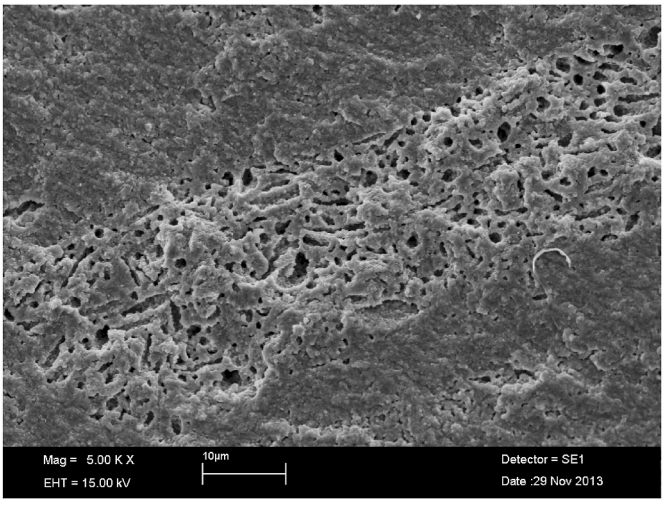

Fig. 10. Photomicrography by SEM of the fracture surface of the Y-TZP/MWCNT-SiO_2 bar-shaped specimen; region with a high concentration of porosity.

Y-TZP was not able to increase its fracture toughness and hardness. In fact, previous studies had already demonstrated that the incorporation of MWCNT in the Y-TZP matrix does not lead to an increase in the hardness of the material (Garmendia et al., 2010a; Zhan et al., 2003; Streicher et al., 2007), which can be considered an advantageous fact for applications in monolithic dental restorations, since an increase in the hardness of the material, it may be associated with greater difficulty in polishing the restoration and rougher surface, thus leading to wear of the natural antagonistic dentition even greater than that caused by a conventional Y-TZP (Sabrah et al., 2013). As to fracture toughness, it was expected that the addition of nanotubes to Y-TZP would result in toughening mechanisms in this material, thus increasing its resistance to crack propagation (Curtin and Sheldon, 2004; Garmendia et al., 2010a; Xia et al., 2004). However, for the composite developed (Y-TZP/MWCNT-SiO_2) this increase in fracture toughness was not verified, which can be attributed to limitations of the test used. The fracture toughness test using a Vickers indentation has been criticized in the literature (Quinn and Bradt, 2007) for being an empirical method that does not provide true values for the fracture toughness of the material. Additionally, the test presents several technical difficulties such as the correct identification of the type of crack that is forming in the material after the indentation. For these reasons, it is difficult to compare the values of fracture toughness obtained for the materials of this study, since there were situations in which crack formation was not observed after indentation in the composite Y-TZP/MWCNT-SiO_2 and, consequently, toughness was not measured in these cases. It is speculated that the absence of cracks in some indentations may be due to toughening by means of crack bridging promoted by the presence of MWCNT-SiO_2 (Curtin and Sheldon, 2004; Xia et al., 2004). As seen in Fig. 9, the composite showed regions of agglomeration of MWCNT-SiO_2 and, in some cases, the indentation may have occurred close to those regions, which prevented the propagation of cracks by the action of the

toughening mechanisms caused by the presence of carbon nanotubes. However, the measured values do not reflect the overall mechanical strength of the material, as fracture toughness tests are carried out producing a controlled defect in the material and do not take into account the defect population existing in the specimen.

The results obtained in the flexural strength test were consistent with what was expected for the conventional Y-TZP. [Ban et al., 2014; Zhang et al., 2004] However, for the Y-TZP/MWCNT-SiO_2 composite, properties were expected to be similar or superior to those obtained for conventional Y-TZP and the results showed that the values found were significantly lower for the composite. This low mechanical performance is directly related to the presence of MWCNT-SiO_2 agglomerates (Fig. 9) and the relatively high level of porosity observed in the composite microstructure (Fig. 10). Alternative processing methods for the experimental composite must be proposed to avoid the formation of these microstructural defects. The use of processing methods with the addition of alcohols in the co-precipitation of mixed hydroxides and the use of deflocculants to aid in the dispersion of MWCNT-SiO_2 coated by mixed oxides in the Y-TZP matrix seem to be the most viable solutions. It is believed that these processing routes that use organic liquids may not affect the final optical properties of the composite, since a subsequent calcination will be proposed with precise temperature control in order to eliminate organic groups adsorbed by the particles of zirconia, without causing the degradation of the MWCNT-SiO_2 structure. However, the effectiveness of this controlled calcination process has yet to be further investigated.

5. Conclusion

The synthesis of a ceramic nanocomposite containing carbon nanotubes (Y-TZP/MWCNT-SiO_2) with appropriate optical properties for making infrastructure for fixed dental prostheses and abutments for implants was possible by means of precursor hydroxide co-precipitation methods, hydrothermal treatment for coating the carbon nanotubes and dispersion of the material obtained in the commercial Y-TZP powder. The methods of co-precipitation and hydrothermal treatment used, despite being viable for making the Y-TZP/MWCNT-SiO_2COOH, need to be optimized in order to avoid the formation of porosities and clusters, which lead to a significant decrease in important mechanical properties of the material, such as flexural strength.

CRediT authorship contribution statement

Lucas Hian da Silva: Writing – review & editing, Writing – original draft, Visualization, Validation, Supervision, Resources, Project administration, Methodology, Investigation, Funding acquisition, Formal analysis, Data curation, Conceptualization. **Laura Ajamil Rinaldi:** Writing – original draft, Methodology, Investigation. **Dolores Ribeiro Ricci Lazar:** Writing – review & editing, Visualization, Validation, Supervision. **Valter Ussui:** Writing – review & editing, Visualization, Validation, Supervision, Methodology. **Rubens Nisie Tango:** Writing – review & editing, Supervision, Conceptualization. **Renan Belli:** Methodology, Investigation, Formal analysis. **Ulrich Lohbauer:** Writing – review & editing, Validation, Supervision, Project administration. **Paulo Francisco Cesar:** Writing – review & editing, Validation, Supervision, Project administration.

Declaration of competing interest

The authors declare that they have no known competing financial interests or personal relationships that could have appeared to influence the work reported in this paper.

Data availability

No data was used for the research described in the article.

Acknowledgements

This work was supported by FAPESP (Fundação de Amparo à Pesquisa do Estado de São Paulo), grants: 2012/10955-5, 2013/00728-4 and 2012/16027-2.

References

Ando, Y., 2010. Carbon nanotube: the inside story. J. Nanosci. Nanotechnol. 10 (6), 3726–3738.
Ban, S., Suzuki, T., Yoshihara, K., Sasaki, K., Kawai, T., Kono, H., 2014. Effect of coloring on mechanical properties of dental zirconia. J. Med. Biol. Eng. 34 (1), 24–29.
Chen, I.W., Xue, L.A., 1990. Development of superplastic structural ceramics. J. Am. Ceram. Soc. 73 (9), 2585–2609.
Curtin, W.A., Sheldon, B.W., 2004. CNT-reinforced ceramics and metals. Mater. Today 7 (11), 44–49.
Dentistry - Ceramic Materials, 2008. ISO 6872 - 2008: International Organization for Standardization.
Garmendia, N., Bilbao, L., Munoz, R., Imbuluqueta, G., Garcia, A., Bustero, I., et al., 2008. Zirconia coating of carbon nanotubes by a hydrothermal method. J. Nanosci. Nanotechnol. 8 (11), 5678–5683.
Garmendia, N., Santacruz, I., Moreno, R., Obieta, I., 2010a. Zirconia-MWCNT nanocomposites for biomedical applications obtained by colloidal processing. J. Mater. Sci. Mater. Med. 21 (5), 1445–1451.
Garmendia, N., Arteche, A., Garcia, A., Bustero, I., Obieta, I., 2010b. The effect of the addition of carbon nanotubes in the hydrothermal synthesis and in the thermal phase stability of nanozirconia. J. Nanosci. Nanotechnol. 10 (4), 2759–2763.
Garmendia, N., Santacruz, I., Moreno, R., Obieta, I., 2012. Influence of the addition of multiwall carbon nanotubes in the sintering of nanostructured yttria-stabilized tetragonal zirconia polycrystalline. Int. J. Appl. Ceram. Technol. 9 (1), 193–198.
Ghinea, R., Perez, M.M., Herrera, L.J., Rivas, M.J., Yebra, A., Paravina, R.D., 2010. Color difference thresholds in dental ceramics. J. Dent. 38 (Suppl. 2), e57–e64.
Hsieh, T.H., Kinloch, A.J., Taylor, A.C., Kinloch, I.A., 2011. The effect of carbon nanotubes on the fracture toughness and fatigue performance of a thermosetting epoxy polymer. J. Mater. Sci. 46 (23), 7525–7535.
Iijima, S., 1991. Helical microtubules of graphitic carbon. Nature 354 (6348), 56–58.
Jagadeesan, D., Eswaramoorthy, M., 2010. Functionalized carbon nanomaterials derived from carbohydrates. Chem. Asian J. 5 (2), 232–243.
Johnson, P.D., 1950. Behavior of refractory oxides and metals, alone and in combination, in Vacuo at high temperatures. J. Am. Ceram. Soc. 33 (5), 168–171.
Kim, M.-J., Ahn, J.-S., Kim, J.-H., Kim, H.-Y., Kim, W.-C., 2013. Effects of the sintering conditions of dental zirconia ceramics on the grain size and translucency. J. Adv. Prosthodont. 5 (2), 161–166.
Larsson, C., Holm, L., Lovgren, N., Kokubo, Y., von Steyern, P.V., 2007. Fracture strength of four-unit Y-TZP FPD cores designed with varying connector diameter. An in-vitro study. J. Oral Rehabil. 34 (9), 702–709.
Lazar, D.R.R., Bottino, M.C., Özcan, M., Valandro, L.F., Amaral, R., Ussui, V., et al., 2008. Y-TZP ceramic processing from coprecipitated powders: a comparative study with three commercial dental ceramics. Dent. Mater. 24 (12), 1676–1685.
Liew, K.M., Wong, C.H., He, X.Q., Tan, M.J., 2005. Thermal stability of single and multi-walled carbon nanotubes. Phys. Rev. B 71 (7), 075424.
Manicone, P.F., Iommetti, P.R., Raffaelli, L., 2007. An overview of zirconia ceramics: basic properties and clinical applications. J. Dent. 35 (11), 819–826.
McLaren, E.A., Giordano, R.A., 2005. Zirconia-based ceramics: material properties, esthetics and layering techniques of a new veneering porcelain, VM9. Quintessence Dent Technol. 28, 99–111.
Mitsias, M.E., Silva, N.R.F.A., Pines, M., Stappert, C., Thompson, V.P., 2010. Reliability and fatigue damage modes of zirconia and titanium abutments. Int. J. Prosthodont. (IJP) 23 (1), 56–59.
Niihara, K., Morena, R., Hasselman, D.P.H., 1982. Evaluation of K_{Ic} of brittle solids by the indentation method with low crack - to - indent ratios. J. Mater. Sci. Lett. 1 (1), 13–16.
Pearce, J.N., Rice, M.J., 1928. The adsorption of water, ethyl alcohol, ethyl acetate, and acetic acid vapors by tungstic and zirconium oxides. Its bearing on heterogeneous catalysis. J. Phys. Chem. 33 (5), 692–704.
Peining, Z., Nair, A.S., Shengyuan, Y., Ramakrishna, S., 2011. TiO2–MWCNT rice grain-shaped nanocomposites—synthesis, characterization and photocatalysis. Mater. Res. Bull. 46 (4), 588–595.
Pittayachawan, P., McDonald, A., Young, A., Knowles, J.C., 2009. Flexural strength, fatigue life, and stress-induced phase transformation study of Y-TZP dental ceramic. J. Biomed. Mater. Res. B Appl. Biomater. 88B (2), 366–377.
Popov, M., Kyotani, M., Nemanich, R.J., Koga, Y., 2002. Superhard phase composed of single-wall carbon nanotubes. Phys. Rev. B 65 (3), 1–4.
Quinn, G.D., Bradt, R.C., 2007. On the vickers indentation fracture toughness test. J. Am. Ceram. Soc. 90 (3), 673–680.
Sabrah, A.H.A., Cook, N.B., Luangruangrong, P., Hara, A.T., Bottino, M.C., 2013. Full-contour Y-TZP ceramic surface roughness effect on synthetic hydroxyapatite wear. Dent. Mater. 29 (6), 666–673.
Standard Test Methods for Determining Average Grain Size Using Semiautomatic and Automatic Image Analysis, 2002. ASTM E 1382 - 1997: American Society for Testing Material Standard.
Streicher, R.M., Schmidt, M., Fiorito, S., 2007. Nanosurfaces and nanostructures for artificial orthopedic implants. Nanomedicine (London, England) 2 (6), 861–874.

Szepesi, C.J., Adair, J.H., 2011. High yield hydrothermal synthesis of nano-scale zirconia and YTZP. J. Am. Ceram. Soc. 94 (12), 4239–4246.
Tinschert, J., Natt, G., Mautsch, W., Augthun, M., Spiekermann, H., 2001. Fracture resistance of lithium disilicate-, alumina-, and zirconia-based three-unit fixed partial dentures: a laboratory study. Int. J. Prosthod. 14 (3), 231–8.
White, S.N., Miklus, V.G., McLaren, E.A., Lang, L.A., Caputo, A.A., 2005. Flexural strength of a layered zirconia and porcelain dental all-ceramic system. J. Prosthet. Dent 94 (2), 125–131.
Xia, Z., Riester, L., Curtin, W.A., Li, H., Sheldon, B.W., Liang, J., et al., 2004. Direct observation of toughening mechanisms in carbon nanotube ceramic matrix composites. Acta Mater. 52 (4), 931–944.
Yoshinori, A., Xinluo, Z., Masato, O., 1998. Sponge of purified carbon nanotubes. Jpn. J. Appl. Phys. 37 (1A), L61.
Yu, M.F., Lourie, O., Dyer, M.J., Moloni, K., Kelly, T.F., Ruoff, R.S., 2000. Strength and breaking mechanism of multiwalled carbon nanotubes under tensile load. Science 287 (5453), 637–640.
Zhan, G.D., Kuntz, J.D., Wan, J., Mukherjee, A.K., 2003. Single-wall carbon nanotubes as attractive toughening agents in alumina-based nanocomposites. Nat. Mater. 2 (1), 38–42.
Zhang, Y., Kim, J.-W., 2009. Graded structures for damage resistant and aesthetic all-ceramic restorations. Dent. Mater. : Off. Publ.Acad.Dent. Mater. 25 (6), 781–790.
Zhang, Y., Pajares, A., Lawn, B.R., 2004. Fatigue and damage tolerance of Y-TZP ceramics in layered biomechanical systems. J. Biomed. Mater. Res. B Appl. Biomater. 71 (1), 166–171.
Zhao, J., Shen, Z., Si, W., Wang, X., 2013. Bi-colored zirconia as dental restoration ceramics. Ceram. Int. 39 (8), 9277–9283.